ORIGINAL ARTICLE

lajss.org© Latin American Journal of Solids and Structures

www.lajss.org

Theoretical and computational simulation of the effect of the number of intermediate diaphragms on the live load distribution factors and structural response of a precast girder bridge

José Miguel Parra Benítez[a], José M. Benjumea[a*], Vladimir Guilherme Haach[b]

[a] Universidad Industrial de Santander, Escuela de Ingeniería Civil, Colombia. Email: jose.parra@correo.uis.edu.co, josbenro@uis.edu.co
[b] Universidade de São Paulo, Escola de Engenharia de São Carlos, Departamento de Estruturas, São Carlos, SP, Brasil. E-mail: vghaach@sc.usp.br

* Corresponding author

https://doi.org/10.1590/1679-78257120

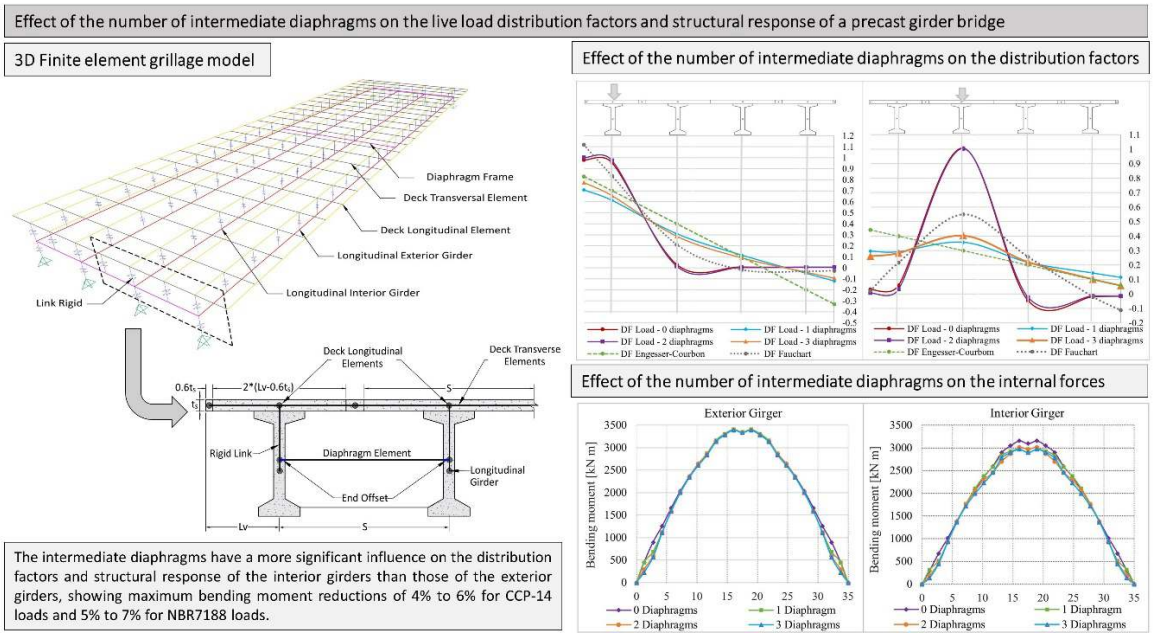
Abstract

Intermediate diaphragms (ID) in bridges with precast girders are intended to improve load distribution among girders. Despite this, their efficacy has been doubted recently due to the complex construction tasks needed to join them to the girders. Accordingly, this work aimed to determine the effect of the number of IDs on the distribution of vertical loads and girders response of a simply supported bridge. Four bridge layouts (0, 1, 2, and 3 IDs) were analyzed using 3D computational grillage models. The load distribution factors from the models were compared to those calculated using the Engesser-Courbon and Fauchart methods to determine the latter's accuracy in capturing the effect of the number of IDs. Moreover, the girders responses under the live loads in the current Colombian and Brazilian bridge design codes were assessed. The results show that the IDs have a more significant effect on the load distribution and deflection of interior girders than the exterior girders. Additionally, increasing the number of IDs reduced the maximum shear and torque while the bending moment and deflections remained nearly constant.

Keywords

Bridge, precast girders, intermediate diaphragms, live load, distribution factors, Engesser-Courbon, Fauchart, finite element method, grillage model.

Graphical Abstract



Received May 20, 2022. In revised form May 23, 2022. Accepted July 20, 2022. Available online July 21, 2022.
https://doi.org/10.1590/1679-78257120

Latin American Journal of Solids and Structures. ISSN 1679-7825. Copyright © 2022. This is an Open Access article distributed under the terms of the Creative Commons Attribution License, which permits unrestricted use, distribution, and reproduction in any medium, provided the original work is properly cited.

1 INTRODUCTION

Bridges built with precast elements can reduce on-site construction time and costs while enhancing the overall quality and durability of the system (Aktan & Attanayake, 2013; Orabi et al., 2016). These advantages have increased the implementation of precast girders in short-to-medium bridges in Latin American countries like Colombia or Brazil (Hällmark et al., 2012; Pacheco et al., 2015; Waimberg et al., 2019). Despite those benefits, the use of prefabricated elements introduces challenges during construction, such as difficulties in the transportation, lifting, and assembly of the precast elements, and other issues associated with the connection between the precast and cast-in-place (CIP) elements (Cai et al., 2007). One example of the latter arises when CIP reinforced concrete (RC) intermediate diaphragms are projected to connect precast girders (Figure 1). This configuration elongates the on-site construction time and may be cumbersome to construct when a scaffolding and wooden construction platform like that shown in Figure 1 is not feasible.

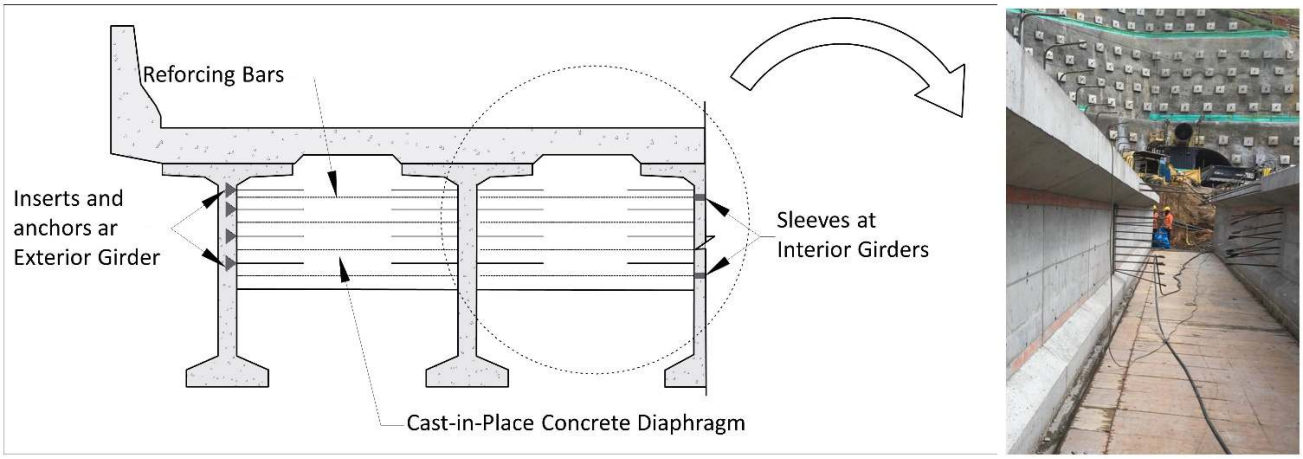


Figure 1. CIP-RC intermediate diaphragms connected to precast girders. Source: left figure modified from PCI, 2003. Right figure: photo taken and provided by Eng. Carlos Castellanos.

According to Dupaquier et al. (2016) and Article 2.3.3.3 of the Reference Manual of the Load and Resistance Factor Design (LRFD) for Highway Bridge Superstructures (AASHTO, 2015), intermediate diaphragms in bridges with precast girders are used to (1) provide temporary stability to the girders during construction until the deck achieves sufficient strength to control the potential lateral-torsional buckling of the girders, (2) improve the distribution among the girders of vertical loads that are applied on the deck and (3) transfer horizontal impact loads between adjacent girders. Despite these functions, the AASHTO-LRFD Bridge Design Specifications (AASvHTO, 2017) equations to determine the moment and shear distribution live load factors do not explicitly include the presence of intermediate diaphragms. This factor and the construction difficulties of CIP intermediate diagrams and their connection to PC elements have led some Department of Transportations in the United States to replace the conventional CIP-RC intermediate diaphragms with steel cross-frames or diaphragms bolted to the web of the girder (Figure 2) or wooden braces used during construction only (Figure 3).

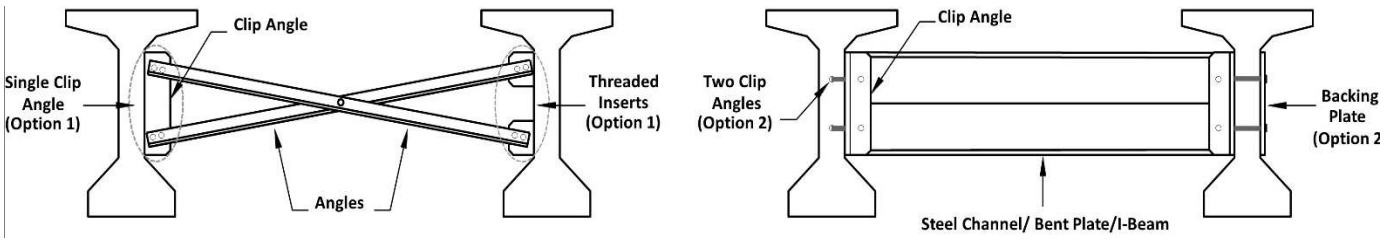


Figure 2. Steel cross-frames and diaphragms for precast girders. Source: modified from Dupaquier et al. (2016).



Figure 3. Temporary wooden cross-frames in Live Oak Bridge in Texas. Source:(PCI, 2011).

From an analytical point of view, intermediate diaphragms have been shown to contribute to the transverse distribution of vertical loads between girders and reduce the superstructure deflections under gravitational loading. This was demonstrated by Cai et al. (2007), who developed finite element (FE) models for two simply supported straight bridges with span lengths of 33.54 m and 39.63 m. In their study, the authors modified the moment transfer capacity (100%, 70%, and 0%) of the connection between the intermediate diaphragms and the girders and found that such parameter significantly affects the superstructure deflection. The authors also noted that the distribution of vertical loads is directly related to the stiffness contribution created by the diaphragms throughout the structure. Green et al. (2004) developed a computational model of an actual bridge with eight precast Florida Bulb-Tee 78" girders connected by two intermediate diaphragms located at the span thirds. The skew angle was varied from 0° to 60°, and the bridge models were analyzed under HL93 loading and constant thermal change. The results showed that the intermediate diaphragms increased the superstructure flexural rigidity by 19% in the straight bridge, 11% in the bridge models with skew angles from 15° to 30°, and 6% in the model with the highest skew. Ma et al. (2007) conducted field tests and calibrated an FE model of a single-span bridge with precast decked bulb-tee girders in Alaska. A particular aspect of that bridge is that the intermediate diaphragms were steel cross-frames like those in Figure 2-b. The measured strains and deflections in the bridge and parametric studies using the FE model showed that the number of cross frames used along the bridge did not significantly affect the distribution factors.

Despite the studies that have been conducted to investigate the effects of intermediate diaphragms in the response of bridges with precast girders, there is currently not enough research that assesses the impact of those elements in bridges with the characteristics and live loads of Latin American countries. Accordingly, this study was aimed to investigate the effect of the number of intermediate diaphragms on the live load distribution factors and structural response of a 35-m long, single-span bridge under the live loads of the Colombian Bridge Design Code, referred to as CCP-14 (AIS, 2014) and the Brazilian Standard of the Brazilian Association of Technical Standards (ABNT, 2013). The investigation was conducted through a parametric analysis using computational models with four configurations of intermediate diaphragms (none, one, two, and three diaphragms). The load distribution factors obtained from the FE models were compared to those calculated using the Engesser-Courbon and Fauchart methods to determine the effectiveness of the latter techniques in capturing the effect of the number of intermediate diaphragms. The responses of the interior and exterior girders (shear force, bending moment, torque, and deflection) were calculated to assess the effect of the number of intermediate diaphragms. It is expected that the results help shed light on the question of whether permanent CIP-RC intermediate diaphragms should be used with precast girders in Latin American countries or if temporary wooden or steel elements be adopted instead.

2 METHODOLOGY

2.1 Bridge characteristics

The study was carried out for a 35-m long, 11.6-m wide concrete girder-slab bridge of a single span (Figure 4). The dimensions of the elements represent the current design and construction practices of these bridges in Colombia. The cross-section of the superstructure consists of four prefabricated I-type girders of depth equal to 1.8 m that are spaced 3 m apart between axes. The girders are connected to a 0.2-m thick reinforced concrete deck slab. The bridge has two

3.65-m wide lanes, two 1.8-m wide shoulders, and New Jersey-type barriers. The girders and intermediate diaphragms were assumed to be constructed with concrete of compressive strength ($f'c$) equal to 35 MPa at 28 days and a modulus of elasticity (E) of 28427 MPa. The latter was calculated using equation 5.4.2.4-1 of the CCP-14. The compressive strength and modulus of elasticity of the deck concrete are 28 MPa and 25426 MPa, respectively. A Poisson ratio of 0.2 was used in the analysis for both types of concrete.

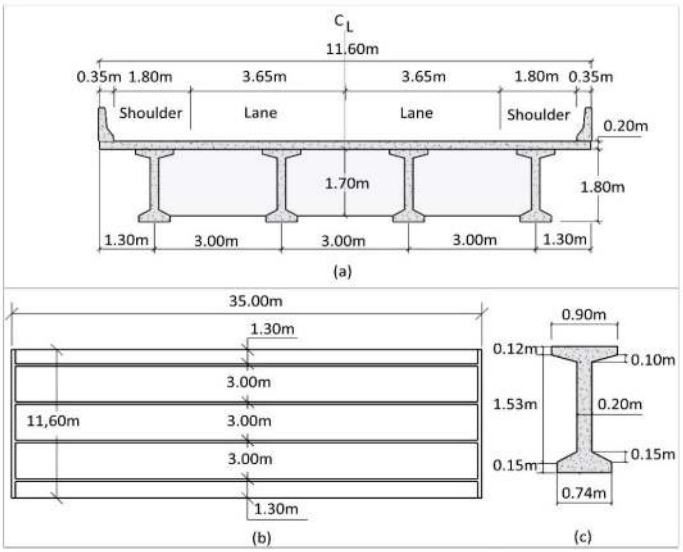


Figure 4. Bridge dimensions: (a) superstructure cross-section, (b) bridge plan view, and (c) girder dimensions.

Figure 5 shows a plan view of the bridge models developed to determine the effect of the number of intermediate diaphragms. The models consist of bridges with none (Bridge N0), one (Bridge N1), two (Bridge N2), and three (Bridge N3) intermediate diaphragms. The diaphragms have a rectangular section of 0.3 m (width) by 1.7 m (depth) and are located symmetrically with respect to the centerline of the bridge. Note that all bridge models have two end-diaphragms in the region of the supports at the abutments, which cross-sectional dimensions were the same as those of the intermediate diaphragms.

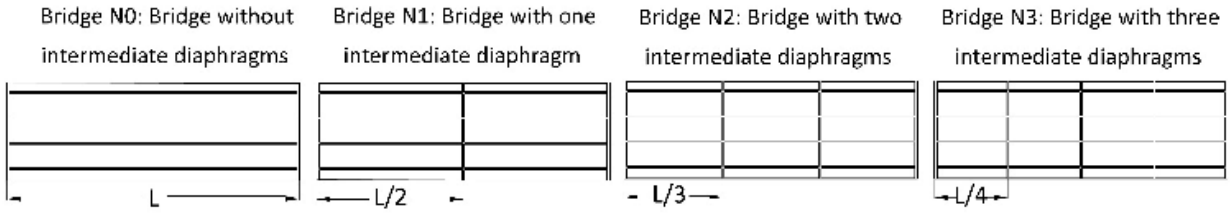


Figure 5. Plan view of the bridge models**.**

2.2 Structural modeling

The computational models of the bridge superstructure were developed using the software SAP2000 V.20 (CSi, 2018). The finite element method (FEM) on which the software is based is widely used to analyze engineering problems composed of systems governed by differential and integral equations. As these equations are not always easy to solve analytically, the FEM divides the problem into several smaller, easier-to-solve elements (Steffen et al., 2018). The computational models used in this study consisted of a 3D grillage formed by several linear beam-column elements (Figure 6-a). The accuracy of the grillage model in determining the structural responses of interest was verified by comparing its results to those determined from a model on which Kringin-based shell elements simulated the deck (Figure 6-b). The Kringin formulation was selected because it captures the potential shear deformations of the deck. The comparison between the two models helped determine the proper discretization of the elements representing the deck in the grillage model. The analysis did not include effects due to transverse inclinations of the superstructure and prestress forces. The responses of the two models under a concentrated load applied at 1/2, 1/3, and 1/4 of the span length (L) were compared, resulting in a maximum difference smaller than 5%. Details of the comparisons can be found

in Parra Benítez (2022). This difference indicated that the grillage model was adequate to investigate the response of the bridge. The description of the grillage model is discussed below.

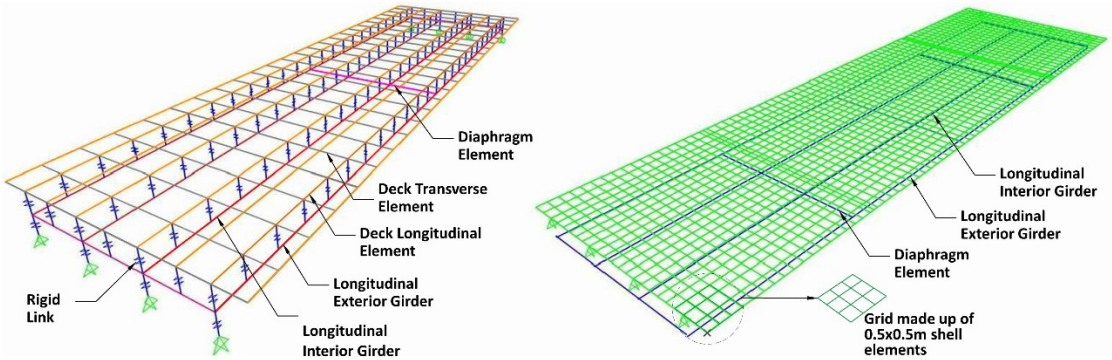


Figure 6. Three-dimensional view of the grillage (a) and shell-based (b) models.

The grillage model was developed following the recommendations by Amirihormozaki et al. (2015) and Cai et al. (2007). The deck was simulated by longitudinal and transverse linear-elastic beam-column (frame) elements located at the deck mid-depth (Figures 6 and 7). The location and cross-section of the longitudinal deck elements were determined based on the tributary width for each girder (Figure 7). Each longitudinal deck element was located on top of each girder, but additional elements were added at the slab edges. As pointed out by Amirihormozaki et al. (2015), it is assumed that the vertical shear flow occurs at $0.3t_s$ from the edge of the deck in solid slabs, where t_s is the deck thickness. Therefore, edge longitudinal deck elements of width $0.6t_s$ were included. The spacing of the deck transverse elements (Figures 6 and 7) was selected to match the spacing between the longitudinal deck elements, forming a squared grillage. Additional deck transverse elements were added at $L/4$, $L/2$ and $L/3$, which are the locations of the intermediate diaphragms. As seen in Figures 6 and 7, the girders are represented by frame elements located at the centroid of the actual I-girder.

Based on the recommendations by Cai et al. (2007), rigid link elements were used to connect the girder elements and the longitudinal deck elements. The intermediate and end diaphragms were modeled by frame elements located at the diaphragm mid-depth (Figure 7), and their connection to the girders was defined as rigid. This was simulated by assigning rigid "end offsets" to the elements that represent the diaphragms (Figure 7).

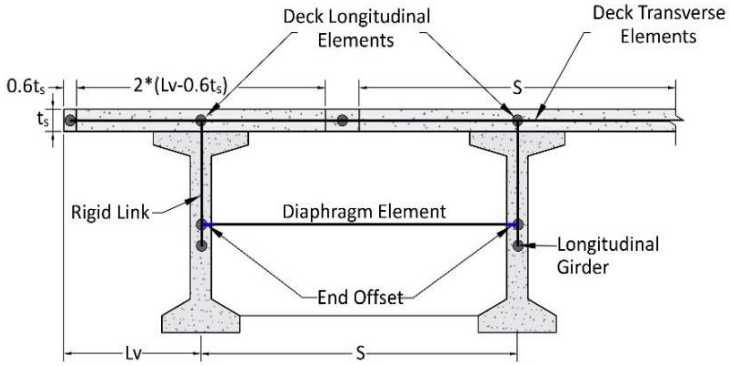


Figure 7. View of longitudinal and transverse elements, tributary width, and their connectivity.

2.3 Calculation of distribution factors

The bridge superstructure consists of a flexible deck and a system of longitudinal girders and transverse girders (diaphragms). The vertical loads applied to the deck are distributed over the superstructure elements based on their relative stiffness. The distribution is determined through the load distribution factors (DF_L), which indicate the percentage of that load taken by each girder at a specific bridge location. The DF allows determining the response of any girder due to loads applied anywhere on the deck. Other distribution factors such as the bending moment (DF_{BM}) and shear (DF_S) factors can also be determined.

The load, shear, and bending moment distribution factors were calculated in this study using the grillage model described in the previous section. The Engesser-Courbon and Fauchart approximate methods were also used to determine the DF_L factors. This allowed estimating their accuracy as the number of intermediate diaphragms changed.

The methodology to calculate the grillage-model-based (computational distribution factors) and approximate distribution factors is as follows.

All distribution factors were calculated at three different cross-sections along the bridge, namely S1 (at L/4), S2 (at L/2), and S3 (at L/3). A unit load (1 kN) was separately applied at six different positions across the deck for each cross-section, as shown in Figure 8. The location of the unit loads corresponded to critical positions on the deck and was sufficient to draw transverse influence lines at each cross-section. The bending moment and shear forces of each composite girder (i.e., girder and deck elements working compositely) were determined using the "Section Cut" tool in SAP2000 at each of the four regions marked with dashed lines in Figure 8. Once those forces were determined, the moment (DF_{BM}) and shear (DF_S) distribution factors for each girder were calculated by dividing the response of interest (bending moment or shear) over the total force in the cross-section being studied.

The load distribution factors (DF_L) were calculated by assuming that each girder in the section corresponds to a flexible support that generates a vertical "reaction" when a unit load is applied to the deck. The reaction was determined by subtracting the composite-girder shear force before and after the section of interest. Then, the DF_L for each girder was calculated as the quotient of the reaction of said girder over the sum of the reactions of all girders.

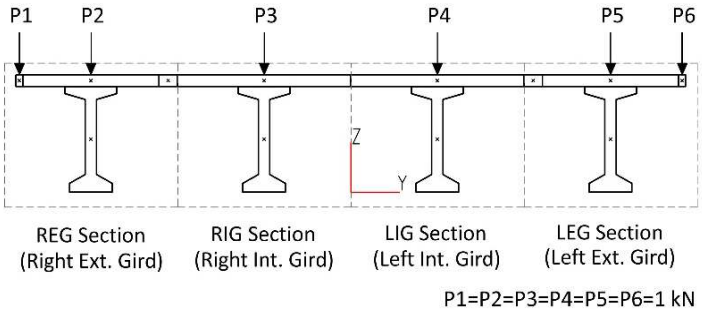


Figure 8. Position of unit loads and regions used for computing composite girders forces.

The Engesser-Courbon method was developed in 1940 for superstructures with parallel girders of constant flexural rigidity joined by an infinitely rigid deck. The method neglects the torsional rigidity of the girders (Alves et al., 2010). Under these hypotheses, the superstructure can be analyzed as a rigid body, and Equation 1 can be used to determine the load distribution factors in each girder (q_i) when a unit load (F) is applied on the deck. In that equation, I_i is the second moment of inertia of the ith girder, x_0 is the horizontal distance from the position of the applied load to the elastic center of the deck cross-section, and X_i corresponds to the horizontal distance between the centroid of the ith girder and the elastic center of the superstructure.

$$q_i = F\left(\frac{I_i}{\sum_{i=1}^{n} I_i} + \frac{x_0 X_i I_i}{\sum_{i=1}^{n} I_i x_i^2}\right) \tag{1}$$

The Fauchart method applies to simply supported, multi-girder superstructures without intermediate diaphragms and with girders of constant inertia. The technique gained popularity because it allows to include the transverse flexibility of the deck (Stucchi, 2006), although the deck longitudinal stiffness is neglected. Fauchart proposed calculating the distribution factors for a planar structure representing a unit-long cross-section of the superstructure. In that model, the girders are replaced by spring supports that partially restrain the vertical displacements and rotations of the deck. The torsional (k_t) and vertical (k_v) stiffnesses of each spring are calculated using Equations 2 and 3, in which E and G are the elastic and shear modulus of the girder, respectively, and I_t is the torsional moment of inertia of the girder. In this study, a 1-m long model of the superstructure cross-section supported on flexible and linear elastic springs was developed, and the distribution factors were then calculated by determining the reactions in each spring due to the application of the point loads shown in Figure 8.

$$k_v = \left(\frac{\pi}{l}\right)^4 EI_i \tag{2}$$

$$k_t = \left(\frac{\pi}{l}\right)^2 GI_t \tag{3}$$

2.4 Calculation of structural responses

The shear, bending moment, torque, and mid-span deflection of the girders under the vehicular live loads were determined for each bridge configuration shown in Figure 5 and further compared. The maximum values from each force envelope were then used to determine the effect of the number of intermediate diaphragms. The responses were obtained for two cases of live loads, one corresponding to that described in the Colombian Bridge Design Code (CCP-14) and the other to the Brazilian ABNT Standard (NBR 7188).

The vehicular live load per lane in CCP-14 comprises six concentrated loads totaling 360 kN plus a uniform distributed load of 3.43 kN/m^2 that acts over a 3-m width region (Figure 9). Each design lane has a width of 3.60 m, meaning that two design lanes were used for the bridge models, given the distance between the interior edges of the barriers (10.9 m). The dynamic amplification factor (IM) and the multi-presence factor (m) were included when calculating the responses of the girders following the recommendations in articles 3.6.2 and 3.6.1.1.2 of CCP-14, which are based on those stated in AASHTO-LRFD Bridge Design Specifications.

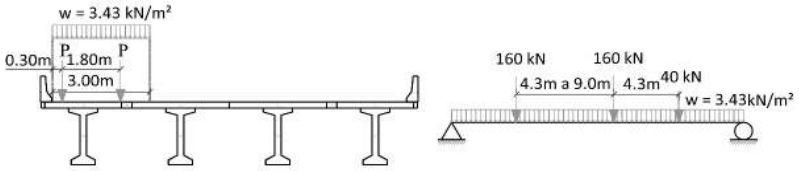


Figure 9. Vehicular live load in CCP-14.
Source: (AIS, 2014)

The vehicular live load of the Brazilian standard NBR 7188 consists of a 450 kN vehicle composed of six wheels (75 kN each) spaced 1.5 m between axles in the longitudinal direction and a uniform load of 5 kN/m^2 (Figure 10). NBR 7188 specifies that the uniform load shall not act in the projected area by the vehicle. For ease of analysis, the distributed load was applied over the entire deck, and the magnitude of the point loads was reduced to 60 kN, resulting in an equivalent loading required by NBR 7188. These loads were amplified by the three factors recommended in the Brazilian standard: coefficient of vertical impact (CIV), coefficient of the number of lanes (CNF), and coefficient of additional impact (CIA). The latter is used to consider the effects due to road discontinuities such as expansion joints, transition structures, and accesses.

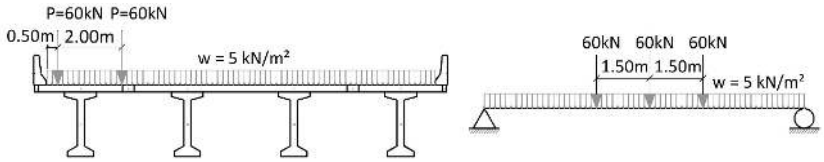


Figure 10. Vehicular live load in NBR7188.
Source: (ABNT, 2013)

3 RESULTS AND ANALYSIS

3.1 Distribution factors

Table 1 presents the maximum values of the load (DF_L), shear (DF_S), and bending moment (DF_{BM}) distribution factors calculated from the grillage model (hereafter referred to as computational distribution factor) and those determined using the approximate methods. The distribution factors are shown for each bridge (N0 to N4), section of study (S1, S2, or S3), and girder type (interior or exterior) analyzed. The relative percentage differences (Diff.) between the approximate and computational distribution factors are shown in Figure 11.

As seen in Table 1 and Figure 11, the results from the Engesser-Courbon method better correlate to the DF_{BM} for both girder types, although this finding is not applicable when the study section coincides with the location of an intermediate diaphragm (i.e., section S2 in bridge N1, section S3 in bridge N2, and sections S1 and S2 in bridge N3). Excluding those sections, the differences between the computational bending moment distribution factors and those determined using the approximate methods range from 8% to 39% and between 1% to 38% in the exterior and interior girders, respectively. In the case of the load and shear distribution factors, the range differences are 27% to 70% and 2% to 69%, respectively. When the study section coincides with the location of an intermediate diaphragm, the Engesser-Courbon method better correlated to the DF_{BM} for the interior girder (differences between 1 and 7%) and the DF_L for the exterior girders (2-127%).

Table 1. Maximum values of the determined distribution factors.

Section	Bridge model	Exterior Girder					Interior Girder				
		Grillage Model			Analytical methods		Grillage Model			Analytical methods	
		DF_L	DF_S	DF_{BM}	Engesser-Courbom	Fauchart	DF_L	DF_S	DF_{BM}	Engesser-Courbom	Fauchart
S1	N0	0.97	0.85	0.65	0.70	0.83	0.95	0.83	0.48	0.30	0.55
	N1	0.97	0.81	0.65			0.95	0.78	0.49		
	N2	0.98	0.71	0.61			0.98	0.59	0.43		
	N3	0.68	0.61	0.55			0.42	0.38	0.32		
S2	N0	0.96	0.98	0.60			1.01	0.98	0.45		
	N1	0.31	0.31	0.32			0.36	0.36	0.30		
	N2	0.98	0.98	0.57			1.00	0.97	0.42		
	N3	0.66	0.66	0.50			0.40	0.40	0.31		
S3	N0	0.96	0.86	0.62			0.94	0.83	0.46		
	N1	0.97	0.78	0.61			0.96	0.71	0.45		
	N2	0.65	0.59	0.52			0.40	0.36	0.31		
	N3	0.99	0.92	0.57			0.98	0.95	0.40		

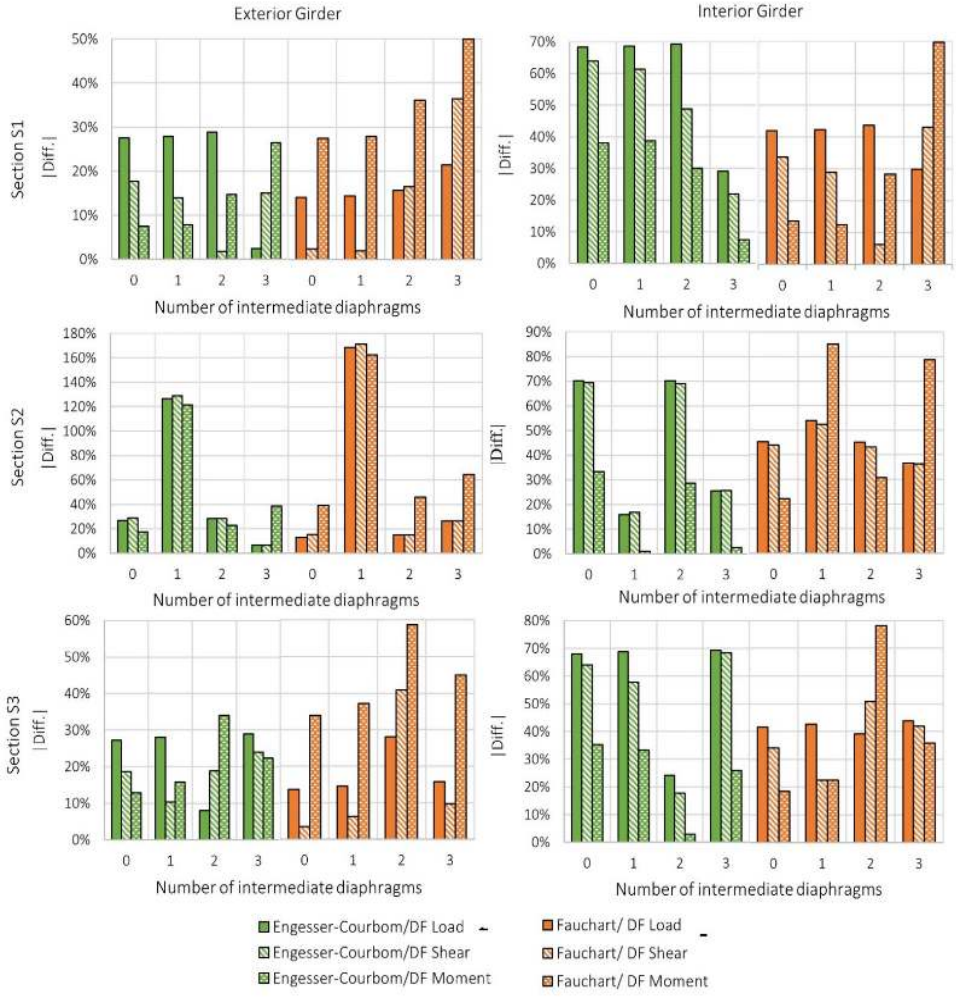


Figure 11. Absolute percentage difference between calculated DFs.

The distribution factors calculated using the Fauchart method differ notably from the computational distribution factors in the cases where the study section coincides with an intermediate diaphragm. As seen in Figures 12 and 13, which present the transverse influence lines for sections S1 and S2 in bridges N3 and N2, that observation is particularly true for the case of interior girders, which help explain the relatively large differences shown in Fig. 11. Except for the cases where there is an intermediate diaphragm in the study section, the method led to a closer correlation to the computational DF_S (2%<Diff.<6%), followed by the DF_L (14%<Diff.<16%) and the DF_{BM} (27%<Diff.<46%) of the exterior girder. This trend is not the same for the interior girder since, in this case, the approximate method correlates better to the computational DF_{BM} (differences between 12 and 36%), followed by DF_S (differences between 6 and 44%) and the DF_L (differences between 42 and 45%). By increasing the number of diaphragms, the precision of the Fauchart method tends to increase in all the study sections, and the study section does not seem to notably affect the degree of correlation of the method with the computational distribution factors.

Table 2 lists the maximum DF_L values as a function of the number of intermediate diaphragms and the study section. The number in parentheses in that table is the percentage difference with respect to the bridge without diaphragms. It is seen that the load distribution factors become smaller in cases where the study section coincides with the position of an intermediate diaphragm, showing reductions with respect to bridge N0 of 29% to 68% for the exterior girder and 55% to 65% for the interior girder. This result confirms that a higher number of intermediate diaphragms in the superstructure improves load distribution among the girders. Figure 14 is used to exemplify the previous statement. That figure presents the transverse influence line for the load DF in the exterior and interior girders at section S2 for all the bridge models. Recall section S2 is a mid-span section, a location of interest for the flexural design. Based on the plots in Figure 14, it can be stated that the reduction of the load DF is inversely proportional to the number of intermediate diaphragms, with the interior girder being more sensitive to the number of intermediate diaphragms.

A higher number of intermediate diaphragms improves the precision of the Engesser-Courbon method with respect to the computational distribution factors. For example, it is seen in Figure 14 that the transverse influence lines for the computational distribution factors tend to be the straight line calculated from the approximate methods. As the number of intermediate diaphragms increases, the differences in the load, shear, and bending distribution factors decrease, as depicted in Figure 11 and Table 2. The lower differences result from the global increase of the flexural stiffness of the bridge with the larger number of diaphragms, which is a closer condition to the infinitely rigid deck assumption in the Engesser-Courbom method.

Table 2. Maximum load DF per study section as a function of the number of diaphragms, with difference relative to bridge N0.

Section	Exterior Girder				Interior Girder			
	N0	N1	N2	N3	N0	N1	N2	N3
S1	1.0	1.0 (0%)	1.0 (0%)	0.7 (30%)	0.9	1.0 (0%)	1.0 (0%)	0.4 (60%)
S3	1.0	1.0 (0%)	0.6 (40%)	1.0 (%)	0.9	1.0 (0%)	0.4 (60%)	1.0 (0%)
S2	1.0	0.3 (70%)	1.0 (0%)	0.7 (30%)	1.0	0.4 (60%)	1.0 (0%)	0.4 (60%)

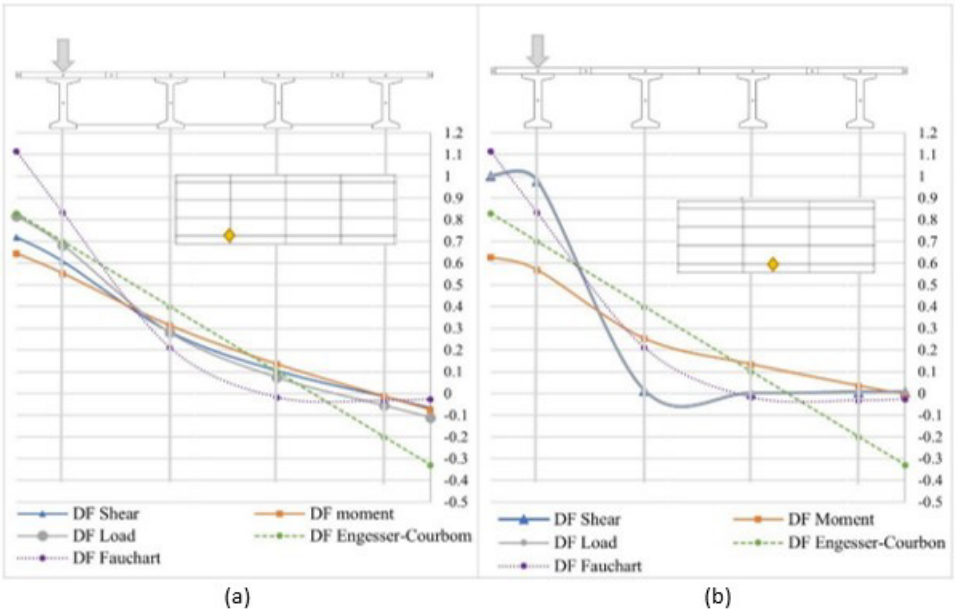


Figure 12. Transverse influence lines for the exterior girder: (a) bridge N3, section S1; (b) bridge N2, section S2

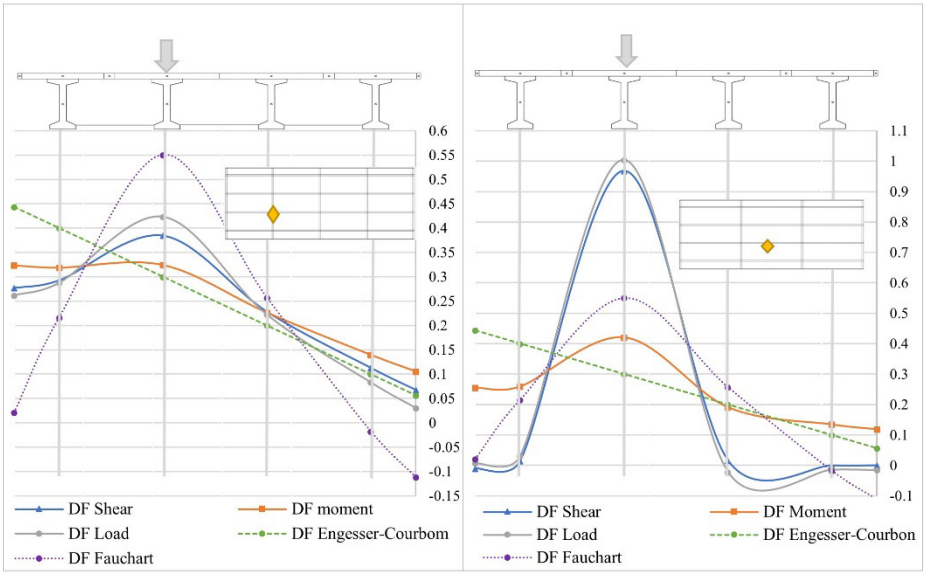


Figure 13. Transverse influence lines of the interior girder, (a) bridge N3, section S1; (b) bridge N2, section S2

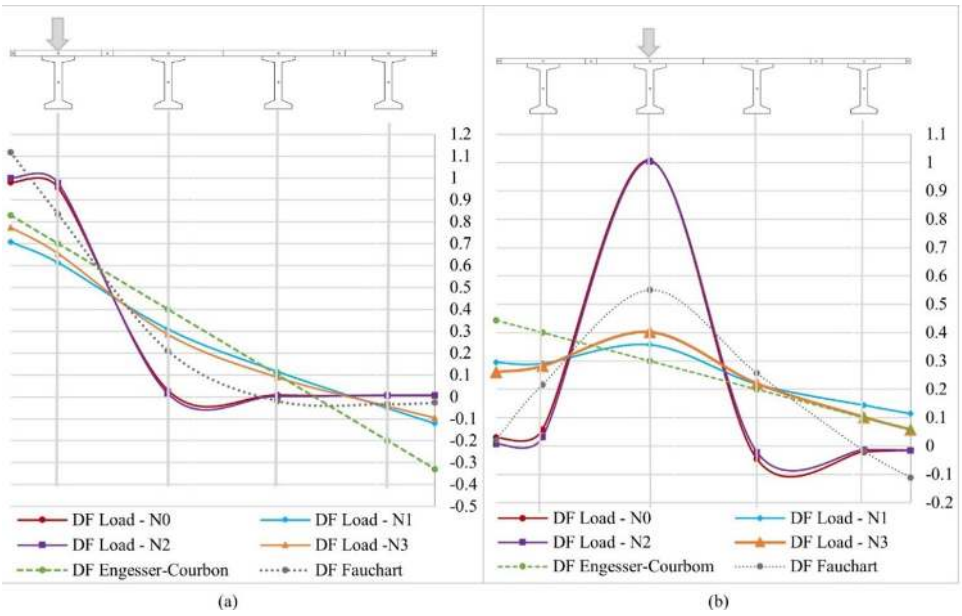


Figure 14. Load transverse influence lines in section S2 for each bridge configuration: (a) exterior girder, (b) interior girder.

3.2 Comparison of Girder Internal Responses and Deflections under Live Load

Figure 15 shows the envelopes for shear force, bending moment, and torque in the girders calculated after applying the CCP-14 vehicular live load described. Maximum values of each envelope are listed in Table 3, while the relative differences of the peak responses relative to those in bridge N0 are shown in Figure 16. Due to space limitations, the envelopes for the NBR7188 live loads are not presented in this paper, although summary results are included. The interested reader can find detailed results for the NBR7188 loads at Parra Benítez (2022).

Based on Figure 15, it is identified that the internal forces and moment envelopes in the interior girders are more sensitive to the presence of intermediate diaphragms than those in the exterior girder. The most significant reduction in both girder types as the number of intermediate diaphragms increased occurs for the torque, with reductions ranging from 10% to 19% (5% to 18% for NBR7188 loads). Shear forces are the second most-affected response, with reductions of 2% to 6% (2% to 4% for NBR7188 loads) and 4% to 12% (1% to 14% for NBR7188 loads) in the exterior and interior girder, respectively. There is a progressive reduction in the maximum values of shear and torque of both beams as the number of intermediate diaphragms increases. However, with the number of diaphragms used in this study (which are reasonable), it cannot be stated to what extent this reduction is no longer noticeable.

Regarding the bending moment, the exterior girder does not have significant reductions due to intermediate diaphragms (0.1% for CCP-14 loads and 1% to 2% for NBR7188 loads). In the interior girder, although there are reductions in said response (4% to 6% for CCP-14 loads and 5% to 7% for NBR7188 loads, Figure 15-b), the decrease is less noticeable as the number of diaphragms increases.

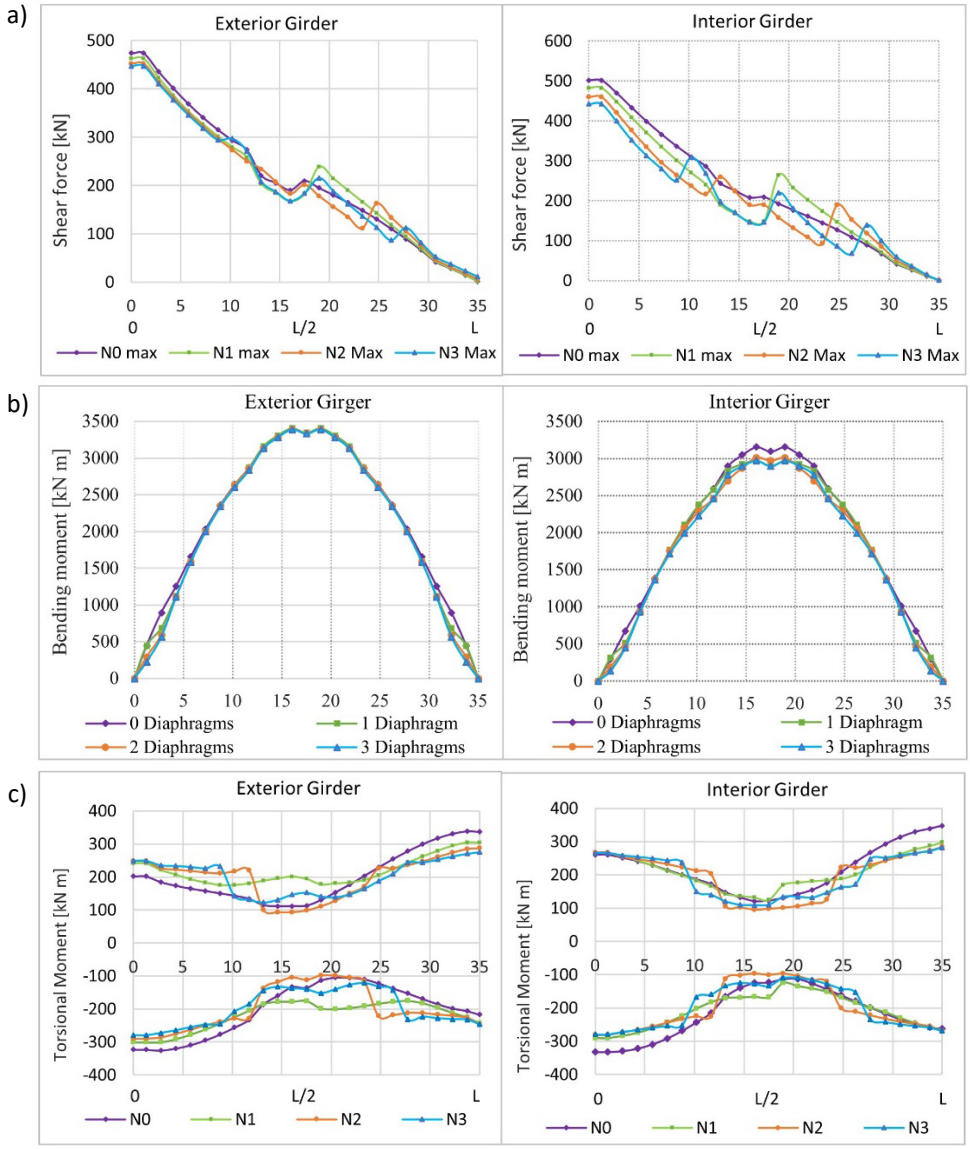


Figure 15. Envelopes of internal responses based on the application of the vehicular load of CCP-14: (a) shear, (b) bending moment, (c) torque.

Table 3. Maximum values of the envelopes of forces and internal moments.

Model	Shear [kN]		Moment [kN m]		Torque [kN m]		Model	Shear [kN]		Moment [kN m]		Torque [kN m]	
	Ext-G	Int-G	Ext-G	Int-G	Ext-G	Int-G		Ext-G	Int-G	Ext-G	Int-G	Ext-G	Int-G
Vehicle load described in CCP-14							Vehicle load described in NBR7188						
N0	474	501	3346	3095	337	348	N0	298	358	2407	2389	159	193
N1	463	482	3342	2900	304	298	N1	304	354	2446	2212	151	169
N2	452	460	3337	2968	288	285	N2	309	346	2415	2281	146	158
N3	447	443	3333	2898	275	283	N3	309	309	2433	2221	140	157

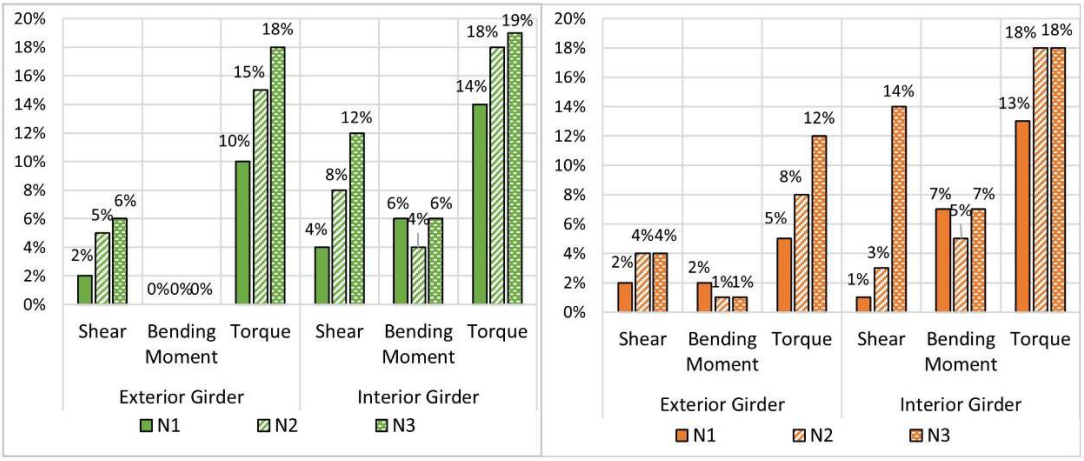


Figure 16. Reduction of internal responses for (a) CCP-14 and (b) NBR7188 live load.

The comparison of the peak structural responses of the bridges with intermediate diaphragms with respect to bridge N0 (Figure 16) shows that the reduction of the internal forces and moments depends on the type of load. This result indicates that the impact of the number of diaphragms depends on the load configuration used in the analysis and design of the bridge superstructure.

It can be identified in Table 3 that the exterior girder controls the flexural design for the live load of the CCP-14, with those moments being approximately 1.08 to 1.15 larger than the bending moments in the interior girder. This is an important factor because CCP-14 requires interior and exterior girders to have the same flexural strength. Thus, any potential reduction in the bending moments of the exterior girders due to the intermediate diaphragms can become valuable in the design. However, as shown in Figure 15 and Figure 16-a, the bending moment in the exterior girders is not affected significantly by the number of intermediate diaphragms. This implies that, although there are bending moment reductions in the interior girders due to the presence of intermediate diaphragms, a significant effect on the design of the girders would not be expected since the exterior girders control the design. As seen in Fig. 16-b, the reductions in the girder bending moments under NBR7188 live loads had a similar trend to those calculated for CCP-14 loads.

Table 4 shows the maximum deflections calculated from the grillage model under vehicular live loads. Both the exterior and interior girders have reductions or increments of less than 1 mm due to the inclusion of intermediate diaphragms. This level of deflection reduction translates into maximum variations of the order of 3%, which are negligible from a practical point of view.

Table 4. Maximum deflection values as a function of the number of diaphragms and the type of live load.

Model	Maximum deflection [cm]		Model	Maximum deflection [cm]	
	Ext Girder	Int Girder		Ext Girder	Int Girder
Vehicle load described in CCP-14			Vehicle load described in NBR7188		
N0	2.72	2.40	N0	1.89	1.76
N1	2.72	2.32	N1	1.90	1.71
N2	2.71	2.31	N2	1.89	1.71
N3	2.71	2.31	N3	1.89	1.70

4 CONCLUSIONS

A 35-m long bridge with four precast girders was analyzed using a 3D grillage model to determine the effect of the number of intermediate diaphragms on the distribution factors (load, moment, and shear) among girders. These factors were compared to those calculated from simplified 2D methods (Engesser-Courbon and Fauchart methods). The effect of the number of intermediate diaphragms on the internal responses of the girders under the live load specified in the Colombian (CCP-14) and Brazilian Bridge Design Codes (NBR7188) was also assessed. Effects inherent to prestress were not considered, and the connection between the intermediate diaphragms and the girders was assumed as rigid. The main conclusions of the study are:

1. Due to simplifications and the assumption of a rigid sectional response, the Engesser-Courbon method does not properly fit a specific distribution factor (load, moment, or shear). This method underestimates those factors in

most cases analyzed in this study, except where the study section coincides with an intermediate diaphragm. The method is more accurate for the exterior girders, and its accuracy increases as the number of diaphragms increases.

2. Except for the study sections that coincide with an intermediate diaphragm, the Fauchart's method has different correlations to the distribution factors calculated from the 3D grillage model, being more precise to the shear force distribution factors in the external girders and to the moment distribution factors in the internal girders. The method precision increases as the number of intermediate diaphragms increases, and the study sections do not notably affect its correlation with the computational distribution factors.

3. The presence of intermediate diaphragms has a more significant influence on the load distribution of the interior rather than exterior girders. When the study section coincides with an intermediate diaphragm, the distribution factors showed a more uniform load distribution among girders. This change in load distribution was independent of the number (≥ 1) of intermediate diaphragms.

4. Increasing the number of intermediate diaphragms generates proportional reductions in the torque and shear responses under live loads of the interior and exterior girders. The exterior and interior girders had reductions in the maximum torque not exceeding 19% for CCP-14 and 18% for NBR7188 loads, while the decrease of maximum shear force in these girders was smaller than 12% for CCP-14 and 14% for NBR loads.

5. The maximum bending moment of the interior girders for the live load in CCP-14 code showed reductions of 4% to 6% when intermediate diaphragms were used. These reductions are not expected to represent a significant change in the flexural design of the girders since the bending moment of the exterior girders governed, and this response remained constant as the number of intermediate diaphragms increased.

6. The maximum bending moment of both girders for the live load in the NBR7188 code showed reductions of 1% to 2% in exterior girders and 5% to 7% in interior girders when intermediate diaphragms were used. The implementation of intermediate diaphragms in the design can positively affect the flexural design of the girders by reducing the maximum bending moment. However, this reduction does not noticeably increase when increasing the number of intermediate diaphragms.

7. From a practical point of view, the variation of the number of intermediate diaphragms has a negligible effect on the deflections under live loading.

5 RECOMMENDATIONS

Considering the study limitations, it is recommended to conduct a more comprehensive analysis to quantify the actual influence of intermediate diaphragms on the distribution of loads and response in the structure. A combination of experimental and analytical studies for several configurations of intermediate diaphragms is required to determine the actual rigidity contribution of the diaphragms to the entire system. This contribution and its modeling should reflect the type of diaphragm (cast-in-place or precast concrete, steel, or wooden diaphragms) and the construction method used.

6 ACKNOWLEDGEMENTS

The authors thank the School of Civil Engineering and the Office of External Relations of Universidad Industrial de Santander for all the arrangements done so that the first author could complete his research stay at the University of São Paulo. Additionally, thanks are due to Vicerrectoría de Investigación y Extension of UIS for the support given through Research Project No. 2823. The third author was supported by Coordenação de Aperfeiçoamento de Pessoal de Nível Superior – Brasil (CAPES) - Finance Code 001 and by CNPq (Brazilian government agency for research – (302479/2017-1).

Author's Contributions: Conceptualization, JM Parra, JM Benjumea and VG Haach; Methodology, JM Parra, JM Benjumea and VG Haach; Investigation, JM Parra; Writing - original draft, JM Parra; Writing - review & editing, JM Benjumea and VG Haach; Funding acquisition, JM Benjumea; Resources, JM Parra, JM Benjumea and VG Haach; Supervision, JM Benjumea and VG Haach.

Editor: Pablo Andrés Muñoz Rojas

References

AASHTO. (2015). Load and Resistance Factor Design for Highway Bridge Superstructures. In M. A. Grubb, K. E. Wilson, C. D. White, & W. N. Nickas (Eds.), *REFERENCE MANUAL* (Vol. 18, Issue 3). AASHTO LRFD Bridge Design Specifications.

AASHTO. (2017). AASHTO LRFD bridge design specifications. In American Association of State Highway and Transportation Officials . (Ed.), *Bridge Engineering Handbook: Fundamentals, Second Edition* (8th ed., Issue September). https://doi.org/10.1201/b15616

ABNT. (2013). NORMA BRASILEIRA ABNT NBR NBR 7188:2013 Carga móvel rodoviária e de pedestres em pontes, viadutos, passarelas e outras estruturas. In *NORMA BRASILEIRA* (p. 64).

Aktan, H., & Attanayake, U. (2013). *Improving Bridges with Prefabricated Precast Concrete Systems.* Western Michigan University. Report No.RC-1602.

Alves, E. V., Almeida, S. M. F. de, & Judice, F. M. de S. (2010). Métodos De Análise Estrutural De Tabuleiros De Pontes Em Vigas Múltiplas De Concreto Protendido. *Engevista, 6*(2), 48–58. https://doi.org/10.22409/engevista.v6i2.138

Amirihormozaki, E., Pekcan, G., & Itani, A. (2015). Analytical modeling of horizontally curved steel girder highway bridges for seismic analysis. *Journal of Earthquake Engineering, 19*(2), 220–248. https://doi.org/10.1080/13632469.2014.962667

Asociación Colombiana de Ingeniería Sísmica. (2014). Norma Colombiana de Diseño de Puentes CCP14. *Norma Técnica, 1*(9), 1689–1699.

Cai, C. S., Chandolu, A., Araujo, M., Chandolu, A., Avent, R. R., Alaywan, W., Dupaquier, S., Marshall, J. D., Stallings, J. M., Luis, J., Sanabria, V., & Martínez, D. M. C. (2007). Diaphragm Effects of Prestressed Concrete Girder Bridges: Review and Discussion. *Practice Periodical on Structural Design and Construction, 12*(2), 48–63. https://doi.org/10.15554/pcij.03012009.48.63

CSi. (2018). *SAP2000 V20. Structural Analysis Program* (No. 22). Computers & Structures Inc.

Dupaquier, S., Marshall, J. D., & Stallings, J. M. (2016). Intermediate Diaphragm and Temporary Bracing Practice for Precast Concrete Girder Bridges. *Practice Periodical on Structural Design and Construction, 21*(2), 04015019. https://doi.org/10.1061/(asce)sc.1943-5576.0000272

Fernando Rebouças Stucchi. (2006). *Pontes E Grandes Estruturas.* Politécnica, Escola Aula, Notas D E Paulo, São.

Green, T., Yazdani, N., & Spainhour, L. (2004). Contribution of Intermediate Diaphragms in Enhancing Precast Bridge Girder Performance. *Journal of Performance of Constructed Facilities, 18*(3), 142–146.

Hällmark, R., White, H., & Collin, P. (2012). Prefabricated Bridge Construction across Europe and America. *Practice Periodical on Structural Design and Construction, 17*(3), 82–92. https://doi.org/10.1061/(ASCE)SC.1943-5576.0000116

Ma, Z., Chaudhury, S., Millam, J., & Hulsey, J. L. (2007). Field Test and 3D FE Modeling of Decked Bulb-Tee Bridges. *Journal of Bridge Engineering, 12*(3), 30–314.

Orabi, W., Mostafavidarani, A., & Ibrahim, M. (2016). *Estimating the Construction Cost of Accelerated Bridge Construction (ABC).* ABC-UTC.

Pacheco, Pedro, Magalhanes, F. (2015). Multi-Span Large Bridges -. *Proceedings of the International Conference on Multi-Span Large Bridges*, 583–590.

Parra Benítez, J. M. (2022). *Análisis de la Influencia del Número de Riostras Intermedias en la Distribución de Carga Variable Vehicular y la respuesta Estructural de un Puente de Vigas Prefabricadas* [Universidad Industrial de Santander]. http://tangara.uis.edu.co/biblioweb/pags/cat/popup/pa_detalle_matbib.jsp?parametros=189772%7C%7C1%7C1

PCI Committee on Bridge. (2003). *Precast prestressed concrete bridge design manual, 2nd edition* (Bridge Design Manual Steering Committee (ed.); 2nd ed., Issue 312). PRECAST/ PRESTRESSED CONCRETE INSTITUTE.

PCI Committee on Bridge. (2011). *Precast prestressed concrete bridge design manual, 3rd edition* (B. D. M. S. Committee (ed.); 3rd ed.). PRECAST/ PRESTRESSED CONCRETE INSTITUTE.

Steffen, L., Oliveira, C., Franzke, P., Figueiredo, D., & Lugarini, T. (2018). *Métodos de Distribuição de Cargas na Seção Transversal de Pontes com Vigamento Múltiplo: Correlação com Resultados Experimentais*.

Waimberg, M., Stucchi, F., Prado, F., & Marquese, M. (2019). The Santos – Guarujá Bridge over Santos Channel. *Structural Integrity, 11*, 655–662. https://doi.org/10.1007/978-3-030-29227-0_71